International Journal of Innovative Computing, Information and Control
Volume **18**, Number **4**, August **2022**

ICIC International ©2022 ISSN 1349-4198
pp. 1133–1145

ROBUST NONLINEAR CONTROL FOR VIRTUAL SYNCHRONOUS GENERATOR BASED ON EXACT FEEDBACK LINEARIZATION

Dezhi Xu*, Ziyang Cheng, Weilin Yang and Weiming Zhang

School of Internet of Things Engineering
Jiangnan University
No. 1800, Lihu Avenue, Wuxi 214122, P. R. China
{ zycheng; wmzhang }@stu.jiangnan.edu.cn; wlyang@jiangnan.edu.cn
*Corresponding author: xudezhi@jiangnan.edu.cn

Received February 2022; revised May 2022

Abstract. *This paper presents a novel secondary control method for voltage regulation in islanded microgrids. Firstly, a large-signal dynamic model of a multi-input multi-output nonlinear system based on a virtual synchronous generator is established, and the multi-input and multi-output nonlinear system is transformed into a completely linear system by means of feedback linearization. The microgrid secondary voltage control is transformed into a linear second-order tracker synchronization problem by feedback linearization. Linear quadratic regulator (LQR) reduces state trajectory deviations with minimal control effort due to their high performance and robustness. The proposed control scheme maintains voltage stability while providing inertia and damping for the microgrid. Finally, the proposed control strategy is evaluated through simulations to demonstrate the effectiveness and robustness of the controller under severe load disturbances, and the results are compared with existing PI controllers.*

Keywords: Virtual synchronous generator, Exact feedback linearization, Microgrid, Linear quadratic regulator

1. Introduction.

The main reason for the ongoing energy transition process in the global economy is the need to protect the environment, especially the climate. Raising public awareness of the destruction of the Earth's ecosystems and technological developments has increased the importance of renewable energy sources as increasingly replacing traditional energy sources. In addition to the environmental aspects, renewable energy offers countries without traditional energy the opportunity to gain greater energy independence and the ability to produce energy. These factors have prompted increasingly decisive action by individual countries and groups to develop renewable energy. The development of renewable energy is a necessary and indispensable process for the sustainable development of individual countries, world regions and even the entire earth [1]. However, the inertia of modern power system decreases with the higher penetration of inverter-connected renewable energy sources and loads. This leads to a low inertia power system that is more sensitive to disturbances and may not be robust enough to survive large disturbances [2].

In terms of power system stability, the inertia means the ability to maintain rotor speed, and frequency under disturbances. In general, the low inertia of power systems will have impact on two key aspects. First, lower inertia results in poorer frequency nadirs when disturbed. If there is not enough kinetic energy to keep the frequency stable at a level, this can lead to large frequency deviations and can be harmful to both the generator and the consumer. In addition, lower inertia results in higher rate of change of frequency, which triggers the active protection system to trip and generate electricity

DOI: 10.24507/ijicic.18.04.1133

[3]. Therefore, it is urgent to save a source for virtual synchrotrons generator (VSG) to compensate for the reduction in conventional sources and keep on the frequency and voltage stability. The main idea of VSG is that an energy storage system with a converter is required to simulate virtual inertia, just like a conventional synchronous generator. VSG can support microgrid operation in island mode to maintain grid frequency when load suddenly changes. [4] proposed a VSG with superconducting magnetic energy storage, which has a faster response speed compared with other energy storage systems. The proposed method provides inertia to modern power systems during unpredictable events and improves frequency and voltage responses. [5] introduced a method to improve island grids with multiple virtual synchronous generators (VSGs) in operation by controlling the input power of the VSG to suppress power fluctuations and reduce the oscillation of the VSG with respect to the system frequency.

The current small-signal models of inverters that mimic synchronous generators usually use the steady-state equation of feeder line and load, and ignore the dynamic characteristics of voltage and current controller of inner loop [6-8]. Global stability is an essential requirement in complex networks. In order to improve the global stability of the controller, it is necessary to establish a large-signal dynamic model for the system [9]. Nonlinear systems can be transformed into linear systems using input-output feedback linearization, which makes it easy to apply well-established linear control techniques to stabilizing the transformed system [10,11]. Robustness is necessary for the stability of a system [12]. After getting a new linear state space model of microgrid. The high performance and robustness of the linear quadratic regulator (LQR) controllers ensure the ability to reduce the deviations in state trajectories with minimum control effort [13-15]. The partial feedback linearization scheme is used to simplify the multi-machine power system [16]. By combining an exact linearization approach and LQR, [17] proposed a novel full-order nonlinear observer-based excitation controller design for interconnected power systems. In order to improve the transient stability of the multi-machine power system, the nonlinear excitation controller design proposed in [18], combined with partial feedback linearization combined with LQR, designed a linear state feedback stabilization controller for the reduced-order linear part. We use LQR to generate optimal parameters of robust nonlinear controller for the state space model of VSG in voltage source three-phase converters for microgrid, to realize and improve the stability and anti-interference performance of the power system. To demonstrate the validity of the proposed control strategy design approach, a simulation model of the island grids with a VSG is constructed.

In this work, we investigate the design of a robust nonlinear controller for virtual synchronous generators in microgrids based on exact feedback linearization. In our method, we first build a large-signal model based on a virtual synchronous generator in order to transform the nonlinear system into a controllable canonical form. Then, the input and output have a linear relationship through the feedback linearization method. Finally, combined with LQR, a controller with secondary voltage control capability for the virtual synchronous generator-based microgrid system is designed.

The rest of this paper is organized as follows. In Section 2, a large-signal nonlinear dynamical model of VSG is introduced. In Section 3, after getting the exact linearization of VSG model, the feedback linearization controller is obtained according to the structure of controller. And to eliminate the voltage deviation generation and to ensure the stable operation of the VSG, the linear optimal control theory is applied in the calculation. In Section 4, simulation results for the microgrid are presented to demonstrate the effectiveness of the proposed controller. Concluding remarks and suggestions for future works are written in Section 5.

2. **A Large-Signal Nonlinear Dynamical Model of VSG.** Figure 1 shows a microgrid control block diagram based on VSG control technology. VSG models can be found in a number of sources. In order to make the inverter have more accurate operation mechanism of synchronous generator, the motion equation of synchronous generator rotor is added in the control part [19]. To design a feedback linearization controller, first of all, the state space model of the system must be obtained. The distributed generation is connected to the microgrid bus by an inverter bridge, and the energy storage is to maintain the VSG direct voltage side voltage constant that is V_{dc}. In order to filter out the effect of high frequency switch on power quality, an LC filter is connected at the inverter output. The mathematical model of the VSG can be formulated as shown in the mechanical part and electrical part. To simulate better the characteristics of synchronous generator, the mechanical part is added in frequency for the inverter bridge. And the electrical part is added to control the voltage amplitude. The selected system state space variable determines the system linearization model by feedback linearization, and controls the output voltage magnitude of the VSG. Then voltage and current dual-loop control ensures voltage stability tracking control performance at inverter outlet [20,21].

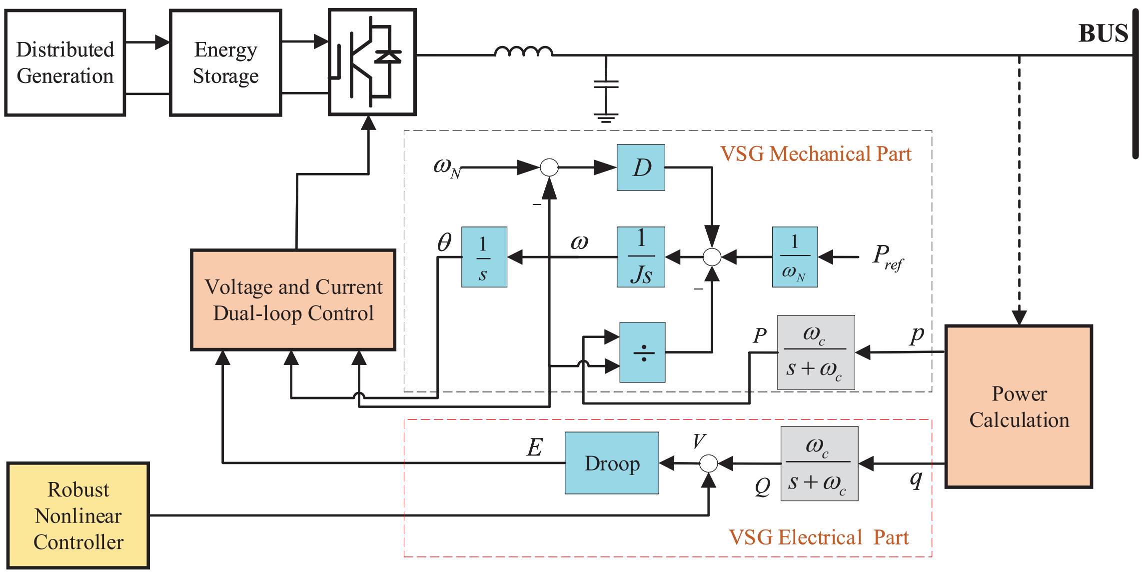

FIGURE 1. Block diagram of a VSG-based MG

In Figure 1, θ is the deviation of the rotational angular frequency ω of the VSG from the rated angular frequency ω_N. D is the virtual damping constant. J is the virtual rotor momentum of inertia constant. P_{ref} is the initial set-point of active power. p and q are the instantaneous power. The mechanical dynamics equation of VSG is as follows:

$$\dot{\theta} = \omega - \omega_N \tag{1}$$

$$\dot{\omega} = -\frac{D}{J}(\omega - \omega_N) - \frac{1}{J}(T_e - T_m) \tag{2}$$

where T_m is the virtual mechanical torque which is assumed to be constant which can be calculated by the initial set-point of power: P_{ref}, and T_e is the virtual electromagnetic torque delivered by active electrical power of the generator. The relationship between torque and active power is as follows:

$$T_m = \frac{P_{ref}}{\omega_N} \tag{3}$$

$$T_e = \frac{P}{\omega_N} \tag{4}$$

where P is the output reactive power of the VSG. To obtain a state space model of the VSG system, each control loop is designed in its dq coordinate system. The dynamic equation of the electrical part of the VSG is as follows:

$$E = U - n(Q - Q_{ref}) \tag{5}$$

where E is the output voltage magnitude of the VSG. U is the control input. n is the droop proportional control gains. Q is the output reactive power of the VSG, and Q_{ref} is the initial set-point of reactive power. P and Q can be obtained via a first-order low-pass filter as follows:

$$\dot{P} = -\omega_c P + \omega_c U_{od} I_{od} + \omega_c U_{oq} I_{oq} \tag{6}$$

$$\dot{Q} = -\omega_c Q + \omega_c U_{oq} I_{od} + \omega_c U_{od} I_{oq} \tag{7}$$

where P is the active power of the VSG, and ω_c is the cut-off frequency of active power low-pass filter. U_{od}, U_{oq} are the direct and quadrature components of VSG's output voltage. I_{od}, I_{oq} are the direct and quadrature components of VSG's output current.

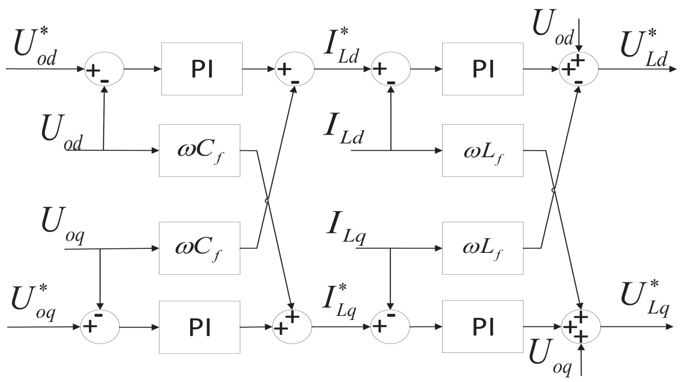

FIGURE 2. Voltage and current control with PI controllers

Figure 2 shows the synchronous reference frame control of the voltages and currents using the PI controllers. In this figure, the voltages and currents are expressed in the synchronous reference frame using transformation [21]. The dynamical models of the voltage controller are written as

$$\begin{cases} I_{Ld}^* = I_{od} + K_{PU}\left(U_{od}^* - U_{od}\right) + K_{IU}\psi_d - \omega_b C_f U_{oq} \\ \dfrac{d\psi_d}{dt} = U_{od}^* - U_{od} \end{cases} \tag{8}$$

and

$$\begin{cases} I_{Lq}^* = I_{oq} + K_{PU}\left(U_{oq}^* - U_{oq}\right) + K_{IU}\psi_q + \omega_b C_f U_{od} \\ \dfrac{d\psi_q}{dt} = U_{oq}^* - U_{oq} \end{cases} \tag{9}$$

where ψ_d and ψ_q are the auxiliary state variables defined for PI controllers. ω_b is the nominal angular frequency. The three-phase voltage output by the VSG is in the rotating coordinate system, the direct-axis component is the peak value of the phase voltage, and the quadrature-axis component is zero. Thus, the U_{od}^* is equal to E, and the U_{oq}^* is equal to 0. C_f is the capacitance value of LC filter. K_{PU} and the K_{IU} are the PI controller coefficients. The dynamical models of the current controller are written as

$$\begin{cases} U_{Ld}^{*} = U_{od} + K_{PI}\left(I_{Ld}^{*} - I_{Ld}\right) + K_{II}\gamma_d - \omega_b L_f I_{Lq} \\ \dfrac{d\gamma_d}{dt} = I_{Ld}^{*} - I_{Ld} \end{cases} \tag{10}$$

and

$$\begin{cases} U_{Lq}^{*} = U_{oq} + K_{PI}\left(I_{Lq}^{*} - I_{Lq}\right) + K_{II}\gamma_q + \omega_b L_f I_{Ld} \\ \dfrac{d\gamma_q}{dt} = I_{Lq}^{*} - I_{Lq} \end{cases} \tag{11}$$

where γ_d and γ_q are the auxiliary state variables defined for PI controllers. The I_{Ld}^{*} and I_{Lq}^{*} are the direct and quadrature components of inverter bridge output current. L_f is the capacitance value of LC filter. K_{PI} and the K_{II} are the PI controller coefficients. By choosing the inductor current of the filter circuit, the capacitor voltage and the filter circuit output current as state variables, and according to Kirchhoff's law and coordinate transformation, the differential equations of the output LC filter and the output connector can be written as

$$\begin{cases} \dot{I}_{Ld} = -\dfrac{R_f}{L_f} I_{Ld} + \dfrac{1}{L_f}\left(U_{Ld} - U_{od}\right) + \omega I_{Lq} \\ \dot{I}_{Lq} = -\dfrac{R_f}{L_f} I_{Lq} + \dfrac{1}{L_f}\left(U_{Lq} - U_{oq}\right) - \omega I_{Ld} \\ \dot{U}_{od} = \omega U_{oq} + \dfrac{1}{C_f}\left(I_{Ld} - I_{od}\right) \\ \dot{U}_{oq} = -\omega U_{od} + \dfrac{1}{C_f}\left(I_{Lq} - I_{oq}\right) \\ \dot{I}_{od} = -\dfrac{R_c}{L_c} I_{od} + \omega I_{oq} + \dfrac{1}{L_c}\left(U_{od} - U_{bd}\right) \\ \dot{I}_{oq} = -\dfrac{R_c}{L_c} I_{oq} - \omega I_{od} + \dfrac{1}{L_c}\left(U_{oq} - U_{bq}\right) \end{cases} \tag{12}$$

where R_f is the total equivalent impedance representing the inductance, line impedance and losses generated during switching of the power tube. R_c and L_c are the output impedance, U_{bd} and U_{bq} are the direct and quadrature components of system output voltage.

3. **Feedback Linearization Controller.** In order to design the proposed feedback linearizing controller, it is necessary to achieve the feedback linearized models. To do this, the dynamics of VSG in the microgrid, as represented by (1)-(12), it is a nonlinear system. The general form of the nonlinear system can be written as

$$\dot{x} = f(x) + g(x)u \tag{13}$$

where $x = \begin{bmatrix} \omega & P & Q & \psi_d & \psi_q & \gamma_d & \gamma_q & I_{Ld} & I_{Lq} & U_{od} & U_{oq} & I_{od} & I_{oq} \end{bmatrix}^T$ are smooth vector fields that are associated to states and u is the input vector. The feedback linearization of the model determines the efficiency of the controller of the microgrid power conversion system, and the feedback linearization characteristic is determined by the relative number of the system, which is determined by the output function [20]. The output function $y = h(x)$ should be selected in such a way that $r = n$. For the mentioned system, the output function is chosen as

$$y = h(x) = U_{od} \tag{14}$$

The mathematical model of the nonlinear system can be linearized using feedback linearization when some conditions as described latter are satisfied. Consider the following nonlinear coordinate transformation

$$z = \phi(x) = \begin{bmatrix} h(x) & L_f h(x) & \cdots & L_f^{r-1} h(x) \end{bmatrix} \tag{15}$$

where $r < N$ is the relative degree corresponding to output function $h(x)$, and $L_f h(x)$ are the Lie derivative [18] of $h(x)$. z and x are the vectors of the same dimension and ϕ is the nonlinear function of x. Now, by nonlinear coordinate transformation, the original x states are transformed into z states. The control input has a state feedback component, the Lie derivates are given by the following equations:

$$L_g h(x) = \frac{\partial h(x)}{\partial x} g(x) = 0 \tag{16}$$

and

$$L_f h(x) = \frac{\partial h(x)}{\partial x} f(x) = \omega U_{oq} + \frac{1}{C_f}(I_{Ld} - I_{od}) \tag{17}$$

and

$$L_g L_f h(x) = \frac{\partial L_f h(x)}{\partial x} g(x) = \frac{K_{PI} K_{PU}}{C_f L_f} \neq 0 \tag{18}$$

where $L_g L_f h(x)$ is the Lie derivative of $L_f h(x)$ along $g(x)$. From the above calculation, it is clear that the relative degree of the system is equal to the order of the system which is 2. Thus, the system is exactly linearizable. The direct coordinates transform is expressed as follows:

$$\begin{cases} \dot{z}_1 = z_2 = L_f h(x) \\ \dot{z}_2 = v = L_f^2 h(x) + L_g L_f h(x) u \end{cases} \tag{19}$$

The linearized system can be expressed as follows

$$\dot{z} = Ax + Bv \tag{20}$$

where

$$A = \begin{bmatrix} 0 & 1 \\ 0 & 0 \end{bmatrix}, \quad B = \begin{bmatrix} 0 \\ 1 \end{bmatrix} \tag{21}$$

To determine the input variable v in (19), v is the "control" input of the linear system of the Brunovsky normal form, so the most reasonable way is using the linear optimal control design method with the quadratic performance index (LQR method) to produce the v. In the linear control system (20), matrices A and B satisfy the following condition, namely the matrix: $D = \begin{bmatrix} B & AB \end{bmatrix}$ has rank 2. This condition means that the system is controllable. The performance index of the system is quadratic.

$$J = \frac{1}{2} \int_0^\infty \left(Z^T \tilde{Q} Z + V^T R V \right) dt \tag{22}$$

where $\tilde{Q}$ is a semi-positive definite weighting matrix, and R is a positive definite weighting matrix. The problem can be granted as obtaining the state feedback vector

$$v = v(Z(t)) = v\begin{pmatrix} z_1 & z_2 \end{pmatrix} \tag{23}$$

which is able to make the performance index J reach its extremum. This is called the LQR problem. When the system is disturbed by the outside world and deviates from the zero state, there is a control v, so that the system target function v to the minimum, then the v is called optimal control. The LQR problem is a constrained variational problem, that is, to find the extremum conditions of the functional J shown in (22). The tracking voltage error of the VSG can be defined as follows:

$$e(t) = Z(t) - Z_R(t) \tag{24}$$

where $Z_R(t) = \left[V_{ref}, \dot{V}_{ref}\right]$, V_{ref} is the target voltage reference. The optimal control is

$$v = -R^{-1}B^T\tilde{P}e(t) = -K(Z(t) - Z_R(t)) \tag{25}$$

where $\tilde{P}$ is the solution of Riccati equation and $K = \left[\begin{array}{cc} k_1 & k_2 \end{array}\right]$ is the linear optimal feedback gain matrix. In order to get the values of $\tilde{P}$ and K, the Riccati algebraic equation needs to be solved:

$$\tilde{P}A + A^T\tilde{P} - \tilde{P}BR^{-1}B^T\tilde{P} + \tilde{Q} = 0 \tag{26}$$

By choosing the weighting matrices $\tilde{Q}$ and R, the value of K can be calculated. Therefore, by using the value of L_gL_fh, L_f^2h and v, the control law can be simplified as

$$u = \frac{-L_f^2h(x) - k_1\left(z_1 - V_{ref}\right) - k_2\left(z_2 - \dot{V}_{ref}\right)}{L_gL_fh(x)} \tag{27}$$

4. **Simulation Results.** Simulation results for the microgrid system were performed using Matlab/Simulink to demonstrate the effectiveness of the system under consideration using feedback linearization controllers, as described in previous sections, for microgrids designed using VSG. The frequency variation, active and reactive power output variation, voltage and current variation of microgrid VSG system under load variation are mainly analyzed. V_{dc} is the DC side voltage, and the V_{rms} is the rated line voltage of the system. The parameters of the large single model system is shown in Table 1.

Table 1. System parameters

Parameter	Value	Parameter	Value
R_f	0.01 Ω	V_{rms}	380 V
ω_N	314 rad/s	V_{dc}	800 V
J	0.1	L_f	1.6 mH
D	4	C_f	700 μF
R_c	0.005 Ω	L_c	1 mH
P_{ref}	8000 W	Q_{ref}	6000 Var
ω_c	70	n	0.003167

The system is in the simulation initialization stage from 0 to 0.2 s, and only the local control system of the inverter is put into operation. At 0.2 s, the system starts to run the control algorithm based on the precise feedback linearized controller. At 0.5 s, the system has a large load connected, and at 1 s, part of the system load is removed. In order to verify the effect of the proposed controller when the load changes after the microgrid is connected. The simulation results are as follows.

Figure 3 shows the change of system frequency in a single VSG microgrid system when the active and reactive loads change simultaneously after the feedback linearization controller is connected to the system at 0.2 s. It can be seen that when the load changes at 0.5 s and 1 s, the frequency change of the system has obvious inertia. The dynamic process is smooth and the oscillation is small, which effectively improves the inertia of the system frequency. Due to the small capacity of the designed system, apparent power is

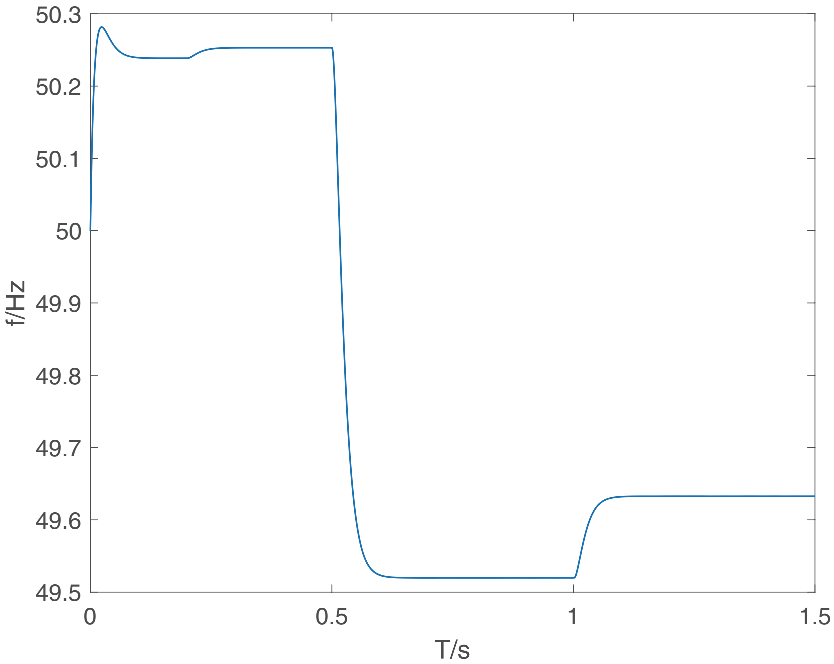

FIGURE 3. Variation of frequency

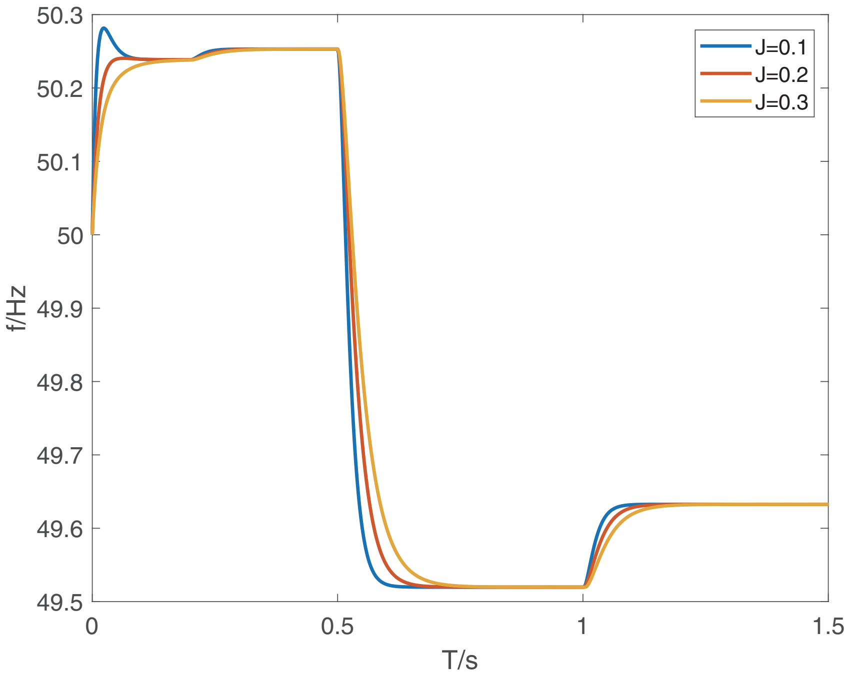

FIGURE 4. Variation diagram of frequency when the value of J is different

10000 VA. When the load changes, the VSG control method keeps the frequency within the range of 50 ± 0.5 Hz. So the frequency fluctuates within the permissible range.

In order to verify that VSG can change the inertia of the system by adjusting J, and change the damping of the system by adjusting D, as shown in Figure 4 and Figure 5, the larger the J, the greater the inertia of the system, and the longer it takes for the system frequency to have the same change. The larger the D is, the greater the system damping is, and the smaller the frequency change is when the load power has the same change.

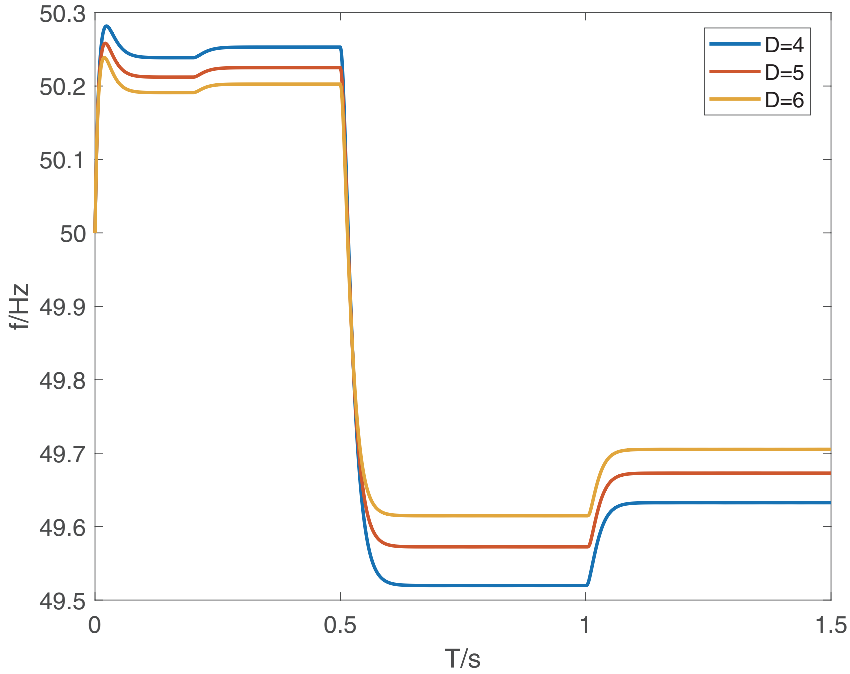

FIGURE 5. Variation diagram of frequency when the value of D is different

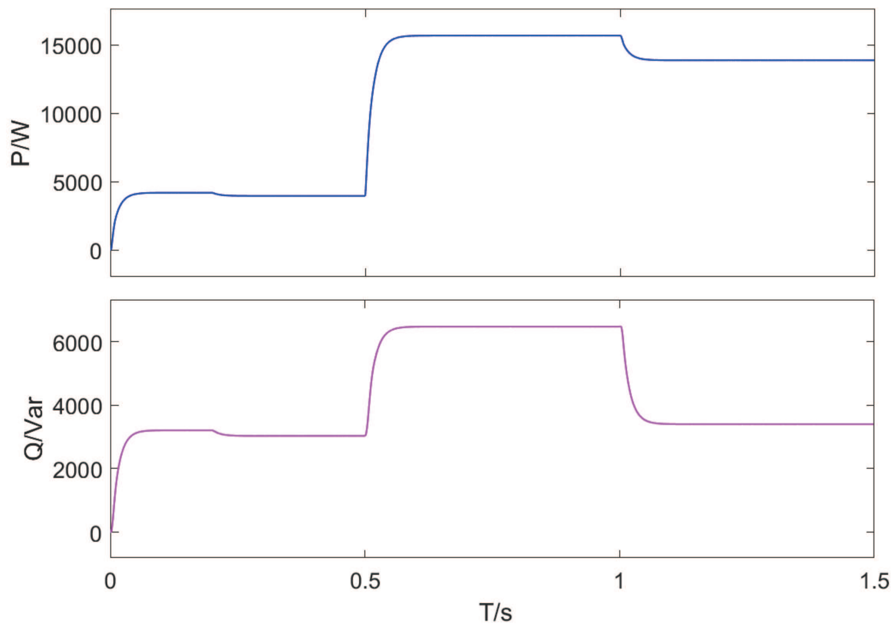

FIGURE 6. Variation of active power and reactive power

Figure 6 exhibits the system power change process when active and reactive loads are added at 0.5 s and then reduced at 1 s. It can be seen that at 0.5 s and 1 s, after the load changes, the variation diagram of active power and reactive power is a smooth curve, indicating that the control strategy can provide enough inertial support capability for the system. It can be seen from Figure 7 that under the feedback linearization control strategy, when the load changes, the voltage waveform remains basically unchanged, and the current waveform changes rapidly. This shows that the system can keep the voltage

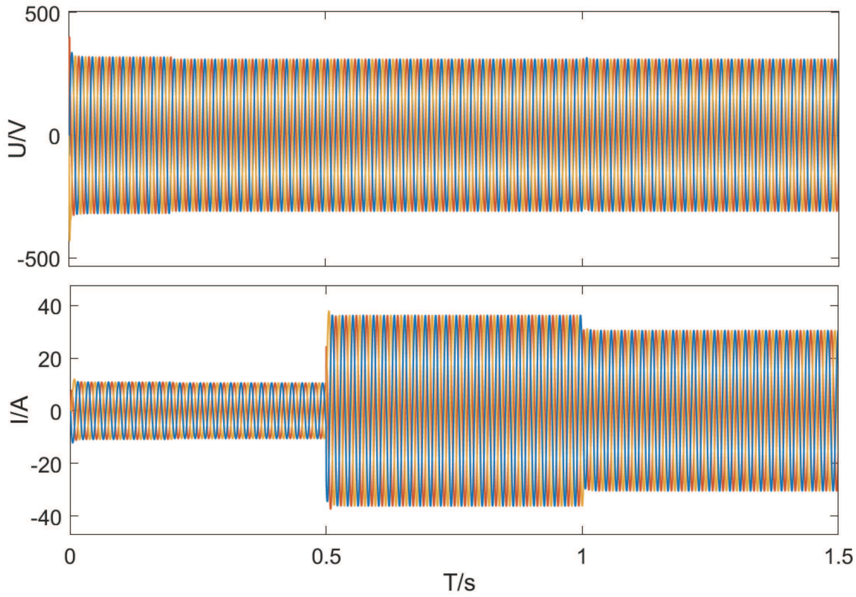

FIGURE 7. Variation of voltage and current

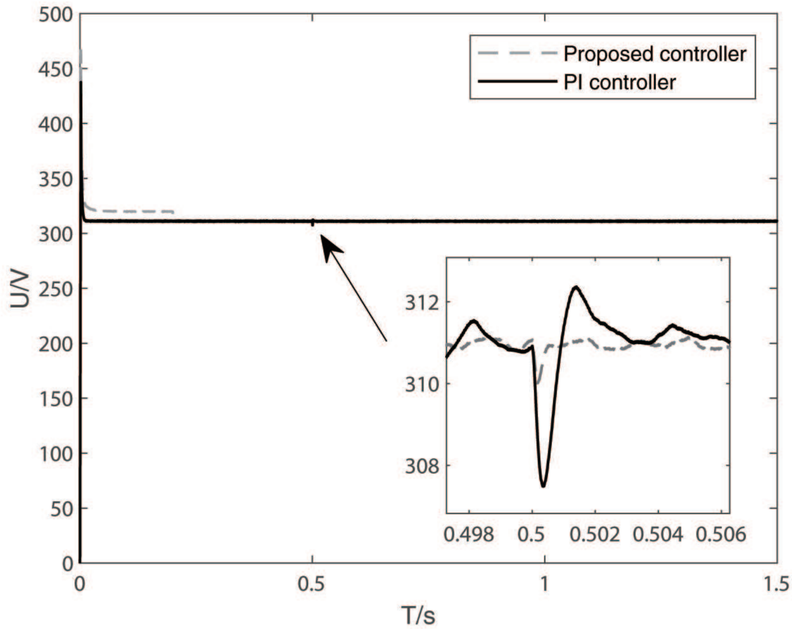

FIGURE 8. Amplitude change of system phase voltage under different controllers

stable when the load changes, so the robust nonlinear control for VSG based on exact feedback linearization has better robustness.

In order to verify the effectiveness of the proposed control method, a comparative test is carried out with the secondary voltage control regulated by the PI controller. The results of the comparison experiment are shown in Figure 8, and it can be clearly seen that the proposed control algorithm is more robust when the load suddenly increases by 300%.

5. **Conclusions.** In order to simplify the nonlinearity of VSG large signal model, this paper adopts Lie derivative to linearize the state feedback of VSG large signal model. The resulting linear model preserves the input and output characteristics. When the nonlinear

power system is completely linearized, a linearized controller is designed. Simulation results show that this strategy can improve the inertia of system output frequency and make the dynamic process smoother. Because LQR is used to obtain the linear optimal feedback gain matrix, it provides robustness to external disturbances. Furthermore, the controller eliminates the disturbance and uncertainty in system parameters which affect system performance. Future work will focus on designing coordination control strategies for multiple VSGs in microgrids.

Acknowledgment. This work is partially supported by the National Natural Science Foundation of China under Grant 61973140, and the Natural Science Foundation of Jiangsu Province under Grant BK20211235. The authors also gratefully acknowledge the helpful comments and suggestions of the reviewers, which have improved the presentation.

REFERENCES

[1] M. Tutak and J. Brodny, Renewable energy consumption in economic sectors in the EU-27. The impact on economics, environment and conventional energy sources. A 20-year perspective, *Journal of Cleaner Production*, vol.345, DOI: 10.1016/j.jclepro.2022.131076, 2022.
[2] L. Ding, Z. Ma, P. Wall and V. Terzija, Graph spectra based controlled islanding for low inertia power systems, *IEEE Trans. Power Delivery*, vol.32, no.1, pp.302-309, 2017.
[3] M. Chen, D. Zhou and F. Blaabjerg, Modelling, implementation, and assessment of virtual synchronous generator in power systems, *Journal of Modern Power Systems and Clean Energy*, vol.8, no.3, pp.399-411, 2020.
[4] H. S. Salama, A. Bakeer, G. Magdy and I. Vokony, Virtual inertia emulation through virtual synchronous generator based superconducting magnetic energy storage in modern power system, *Journal of Energy Storage*, vol.44, DOI: 10.1016/j.est.2021.103466, 2021.
[5] M. Choopani, S. H. Hosseinain and B. Vahidi, A novel comprehensive method to enhance stability of multi-VSG grids, *International Journal of Electrical Power & Energy Systems*, vol.104, pp.502-514, 2019.
[6] B. Zhang and J. Zhang, Small-signal modeling and analysis of a three-phase virtual synchronous generator under off-grid condition, *Energy Reports*, vol.8, Supplement.1, pp.1200-1207, 2022.
[7] Z. N. Sun, D. Z. Ma and S. Li, An oscillation damping method for frequency-detector-less virtual synchronous generators, *Energy Reports*, vol.7, Supplement.7, pp.1485-1494, 2021.
[8] X. F. Wan, X. H. Ding, H. L. Hu and Y. J. Yu, An enhanced second-order-consensus-based distributed secondary frequency controller of virtual synchronous generators for isolated AC microgrids, *Energy Reports*, vol.7, pp.5228-5238, 2021.
[9] G. N. Lou, W. Gu, W. X. Sheng, X. H. Song and F. Gao, Distributed model predictive secondary voltage control of islanded microgrids with feedback linearization, *IEEE Access*, vol.6, pp.50169-50178, 2018.
[10] B. H. K. Konan, K. Hashikura, M. A. S. Kamal and K. Yamada, Approximate state feedback linearization for MIMO systems, *ICIC Express Letters*, vol.14, no.7, pp.679-685, 2020.
[11] A. S. Elkhatem and S. N. Engin, Robust LQR and LQR-PI control strategies based on adaptive weighting matrix selection for a UAV position and attitude tracking control, *Alexandria Engineering Journal*, vol.61, no.8, pp.6275-6292, 2022.
[12] S. Sarakon, T. Phoka and K. Tamee, Robust noise for human activity recognition using convolutional neural network, *ICIC Express Letters, Part B: Applications*, vol.11, no.3, pp.229-236, 2020.
[13] N. Agrawal, S. Samanta and S. Ghosh, Modified LQR technique for fuel-cell-integrated boost converter, *IEEE Trans. Industrial Electronics*, vol.68, no.7, pp.5887-5896, 2021.
[14] L. Fan, P. Liu, H. Teng, G. Q. Qiu and P. Jiang, Design of LQR tracking controller combined with orthogonal collocation state planning for process optimal control, *IEEE Access*, vol.8, pp.223905-223917, 2020.
[15] Q. M. Li and M. E. Baran, A novel frequency support control method for PV plants using tracking LQR, *IEEE Trans. Sustainable Energy*, vol.11, no.4, pp.2263-2273, 2020.
[16] T. F. Orchi, T. K. Roy, M. A. Mahmud and A. M. T. Oo, Feedback linearizing model predictive excitation controller design for multimachine power systems, *IEEE Access*, vol.6, pp.2310-2319, 2018.

[17] M. A. Mahmud, H. R. Pota and M. J. Hossain, Full-order nonlinear observer-based excitation controller design for interconnected power systems via exact linearization approach, *International Journal of Electrical Power & Energy Systems*, vol.41, no.1, pp.54-62, 2012.
[18] M. A. Mahmud, H. R. Pota, M. Aldeen and M. J. Hossain, Partial feedback linearizing excitation controller for multimachine power systems to improve transient stability, *IEEE Trans. Power Systems*, vol.29, no.2, pp.561-571, 2014.
[19] Q. C. Zhong and G. Weiss, Synchronverters: Inverters that mimic synchronous generators, *IEEE Trans. Industrial Electronics*, vol.58, no.4, pp.1259-1267, 2011.
[20] M. A. Mahmud, M. J. Hossain and H. R. Pota, Selection of output function in nonlinear feedback linearizing excitation control for power systems, *2011 Australian Control Conference*, Melbourne, VIC, Australia, pp.458-463, 2011.
[21] A. Keyhani, M. N. Marwali and M. Dai, *Integration of Green and Renewable Energy in Electric Power Systems*, Wiley, Hoboken, NJ, USA, 2010.

Author Biography

Dezhi Xu received the Ph.D. degree in control theory and control engineering from Nanjing University of Aeronautics and Astronautics, China, in 2013.

Dr. Xu was a Visiting Fellow with the Department of Biomedical Engineering, City University of Hong Kong, Hong Kong, from 2018 to 2019. He joined Jiangnan University from 2014, as an Associate Professor. His current research interests include data driven control, fault diagnosis and fault-tolerant control, multi-agent systems and CPSs, technologies of renewable energy, motor control, and smart grid.

Dr. Xu was a recipient of the First Class Award of Science and Technology Progression from the China General Chamber of Commerce in 2016 for his research results. He is a Committee Member of the Association of Energy Internet, and Trusted Control of the Chinese Association of Automation (CAA), and Committee Member of energy storage of the China Renewable Energy Society (CRES).

Ziyang Cheng received the B.S. degree in electrical engineering and automation from Harbin Institute of Technology, China, 2017. He is currently working toward the M.S. degree in electrical engineering with Jiangnan University, Wuxi, China. His current research interests include virtual synchronous generator control strategy.

Weilin Yang received the B.Eng. degree in machine design, manufacturing and automation from the University of Science and Technology of China, Hefei, China, in 2009, and the Ph.D. degree in mechanical engineering from the City University of Hong Kong, Hong Kong, in 2013.

Dr. Yang was a Post-Doctoral Researcher with the Masdar Institute of Science and Technology (now Khalifa University), Abu Dhabi, United Arab Emirates, from 2013 to 2016. He was a Research Engineer with General Electric (GE) Global Research, Shanghai, China, from 2016 to 2017. He has been an Assistant Professor with Jiangnan University, Wuxi, China, since 2017. His research interests include modeling and control of motor and energy systems, and computational fluid dynamics.

Weiming Zhang received his M.S. degree in control engineering from Jiangnan University, Wuxi, China in 2020. He is currently working toward the Ph.D. degree in control engineering with Jiangnan University, Wuxi, China. His current research interests include data-driven control, model-free adaptive control and multiagent systems.